

Supplementary Information

Loss of epidermal microRNA-149 sensitizes to skin inflammation

Longlong Luo^{1,2,3*}, Hao Yuan⁴, Ankit Srivastava^{3,6}, Karl Annusver⁴, Nupur Khera³, Piyal Saha³, Roxane Prioux³, Kunal Das Mahapatra³, Evelyn Kelemen^{1,2}, Menil Dholakia^{1,2}, Jan Cedric Freisenhausen^{1,2,3}, Milena Petkova⁵, Taija Mäkinen⁵, Gunnar Pejler², Maria Kasper⁴, Andor Pivarcsi^{2,3}, Enikő Sonkoly^{1,2,3*}

¹Dermatology and venereology, Department of Medical Sciences, Uppsala University, Uppsala, Sweden

²Department of Medical Biochemistry and Microbiology (IMBIM), Uppsala University, Uppsala, Sweden

³Dermatology and Venereology Division, Department of Medicine Solna, Karolinska Institutet, Stockholm, Sweden

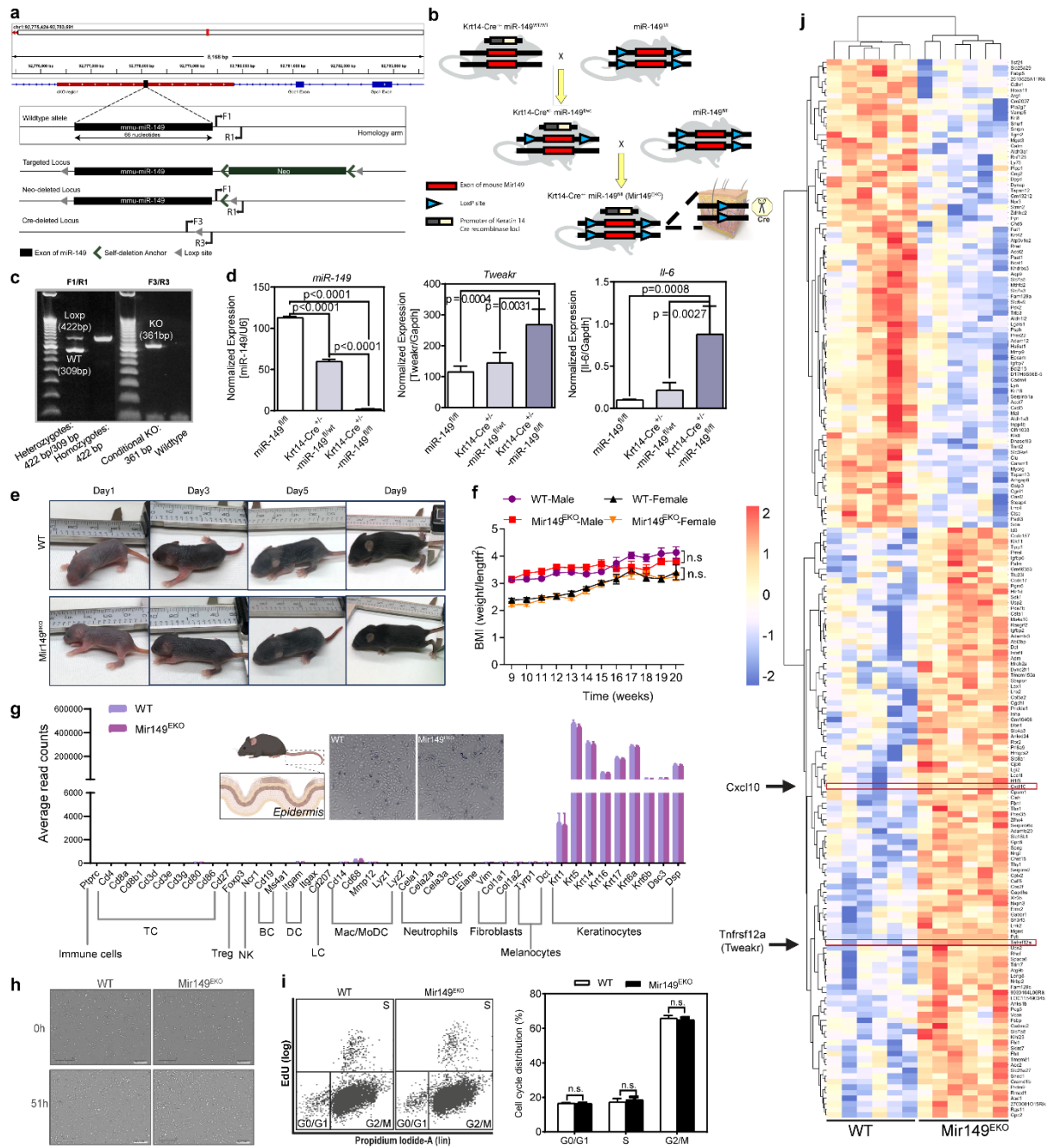
⁴Department of Cell and Molecular Biology, Karolinska Institutet, Stockholm, Sweden

⁵Department of Immunology, Genetics and Pathology, Vascular Biology, Uppsala University, Uppsala, Sweden

⁶The Program in Epithelial Biology, Stanford University School of Medicine, Stanford, California, USA

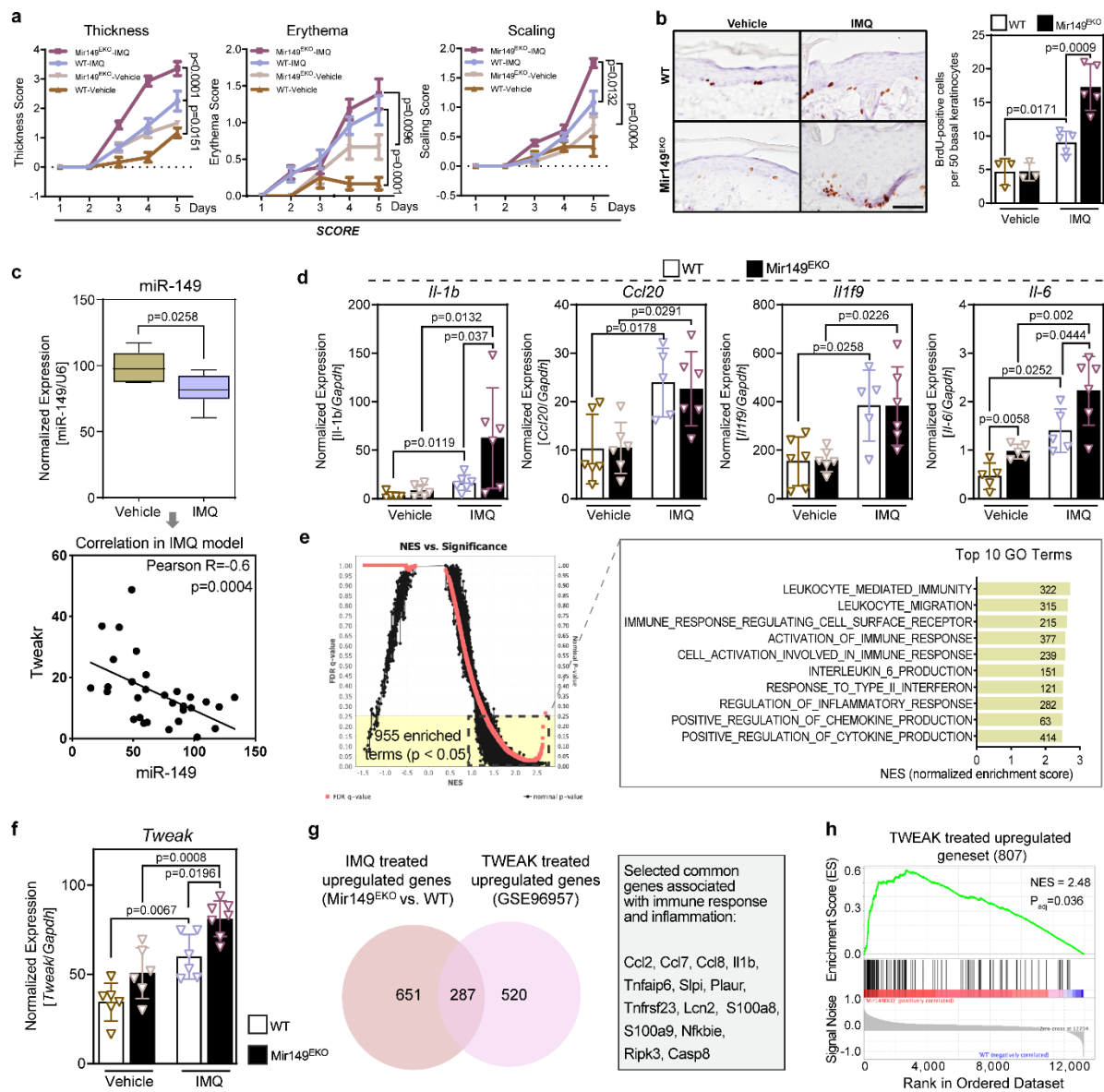
***Corresponding author:** Enikő Sonkoly and Longlong Luo

Supplementary Figure 1.



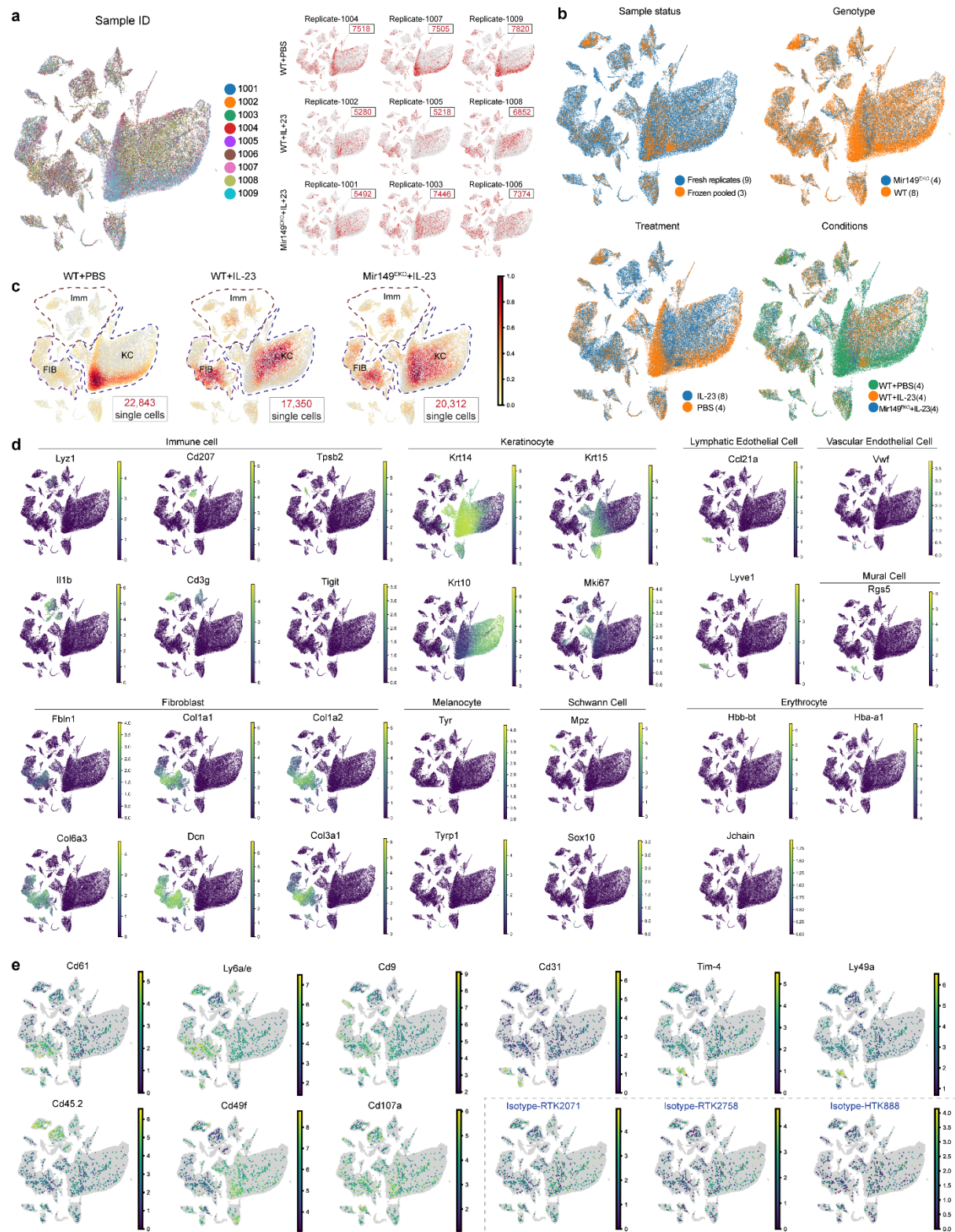
Supplementary Figure 1. Generation and characterization of epidermis-specific miR-149 knockout mice. **a.** Schematic representation of genotyping primers and targeting strategy. **b.** Conditional knockout model of miR-149 in epidermal basal keratinocytes generated by crossing *Mir149^{fl/fl}* mice with Krt14-Cre mice. **c.** miR-149 genotyping with F1/R1 and F3/R3 primers, showing 422 bp band for WT and 361 bp for knockout alleles. **d.** qRT-PCR analysis of miR-149, Tweakr, and Il-6 expression in epidermis from WT and *Mir149^{EKO}* mice. **e.** Skin phenotypic progression in WT and *Mir149^{EKO}* mice from day 1 to day 9. **f.** Body mass index (BMI) of WT and *Mir149^{EKO}* mice from 9 to 20 weeks (n = 6). **g.** Representative images and marker gene expression in keratinocytes isolated from WT and *Mir149^{EKO}* mice. **h.** IncuCyte live-cell analysis of primary keratinocyte growth (n = 6). **i.** EdU cell cycle assay analysis of cell cycle progression (n = 6). **j.** Unsupervised heatmap of gene expression differences between *Mir149^{EKO}* and WT mice (n = 6). The data were analyzed by one-way ANOVA (**d**) and unpaired two-tailed student's t-test (**i**). Data are presented as mean ± SD (**d, g, i**) or mean ± SEM (**f**). Source data are provided as a Source Data file.

Supplementary Figure 2.



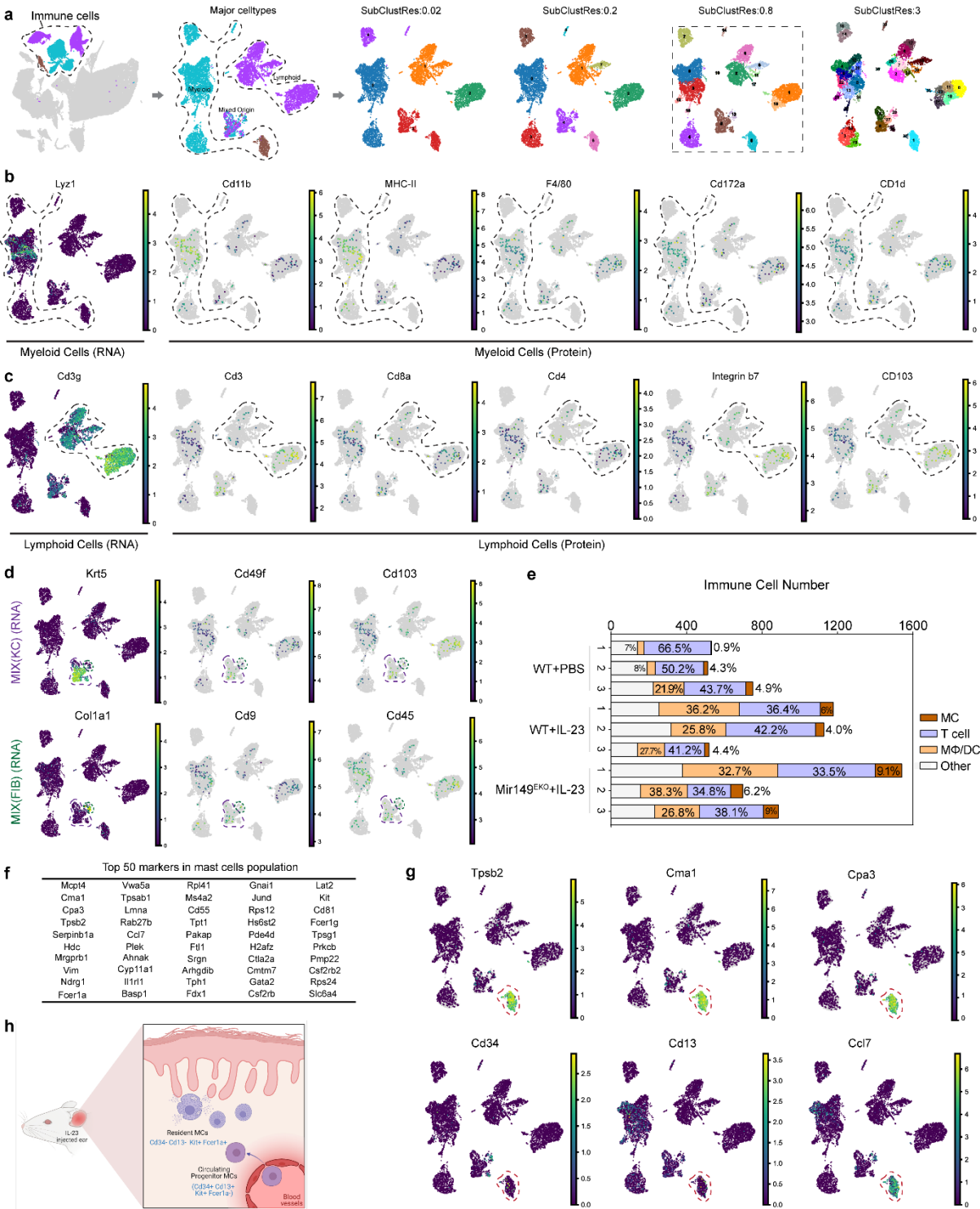
Supplementary Figure 2. Deletion of *Mir149* in the epidermis exacerbates IMQ-induced psoriasis-like skin inflammation and induces transcriptomic changes with enrichment of a TWEAK-associated signature. **a.** Severity scores for skin thickness, erythema, and scaling in IMQ-treated *Mir149^{EXO}* (n=7) and WT (n=6) mice. **b.** BrdU incorporation (brown) indicates increased epidermal proliferation in IMQ-treated *Mir149^{EXO}* mice. **c.** qRT-PCR for miR-149 in IMQ-treated WT skin and a negative correlation between Tweakr and miR-149 in an extended cohort of mouse skin samples from the IMQ model. **d.** qRT-PCR for psoriasis-associated inflammatory mediators (Il-1b, Ccl20, Il1f9, Il-6) (n = 6-7). **e.** GSEA identifies 955 upregulated gene sets in IMQ-treated *Mir149^{EXO}* skin, with the top 10 shown. **f.** qRT-PCR for Tweak expression in vehicle or IMQ-treated WT (n = 6) and *Mir149^{EXO}* (n = 7) skin. **g.** Intersection analysis of Tweak-upregulated genes (GSE96957) and DEGs from IMQ-treated *Mir149^{EXO}* skin, highlighting 8 common genes. **h.** GSEA shows enrichment of TWEAK-upregulated gene sets in IMQ-treated *Mir149^{EXO}* skin. The data were analyzed by unpaired two-tailed student's t-test (**c**) and one-way ANOVA (**b**, **d**, **f**) and two-way ANOVA (**a**). Data are presented as mean \pm SD (**b-d**, **f**) or mean \pm SEM (**a**). Scale bar = 50 μ m. Source data are provided as a Source Data file.

Supplementary Figure 3.



Supplementary Figure 3. Single-cell analysis of cell distribution, marker gene expression, and surface protein profiling among major cell populations after the first level of clustering. **a.** UMAP plot for all cells from nine mouse samples, shown together or separately, with cell numbers from each sample indicated. **b.** UMAP plot showing batch effects across sample status, genotype, treatment, and conditions. **c.** Feature plot visualizing immune population distribution among WT cells with PBS or IL-23 and *Mir149*^{EKO} cells with IL-23. **d.** Feature plot showing expression of marker genes for immune cells, keratinocytes, fibroblasts, melanocytes, Schwann cells, mural cells, endothelial cells, and erythrocytes. **e.** Distribution of selected cell surface proteins (Cd61, Ly6a/e, Cd9, Cd31, Tim-4, Ly49a, Cd45.2, Cd107a) along with 3 isotype controls. Source data are provided as a Source Data file.

Supplementary Figure 4.



Supplementary Figure 4. Single-cell transcriptome and cell surface protein expression reveal the distribution of immune cells in control or IL-23-injected ear skin. **a.** UMAP plot visualization depicting the process of sub-clustering for all immune cell populations at varying resolutions, with 0.8 highlighted as the final chosen resolution. **(b-d).** Feature plot displaying the expression of selected RNA markers (Lyz1, Cd3g, Krt5, Col1a1) and cell surface proteins in two major lineages: myeloid (Cd11b, MHC-II, F4/80, Cd172a, and Cd1d) and lymphoid cells (Cd3, Cd8a, Cd4, Integrin β 7, and Cd103), as well as two mixed populations (Cd49f, Cd103, Cd9, Cd45). **e.** Bar plot quantifying cell numbers and proportions of mast cells, macrophages/dendritic cells, and T cells from individual donors. **f.** Table showing the top 50 makers for mast cells. **g.** Feature plot displaying the expression of selected RNA markers (Tpsb2, Cma1, Cpa3, Cd34, Cd13, Ccl7) within mast cells. **h.** Illustration graph showing the resident mast cells and bloodstream derived progenitor mast cells in IL-23 injected ear skin. Source data are provided as a Source Data file.

a

Vehicle+PBS Vehicle+Monensin IMQ+PBS IMQ+Monensin

Day1
Day2
Day3
Day4

b

Weight Erythema Scaling Thickness

Normalized Weight change Erythema Score Scaling Score Thickness Score

Time (days)

PBS-Vehicle Monensin+Vehicle PBS-IMQ Monensin+IMQ

c

PBS Monensin

Vehicle IMQ

Toluidine blue

Toluidine blue⁺ cells per field

Vehicle IMQ

PBS Monensin

d

PBS Monensin

Vehicle IMQ

H&E staining

Epidermal Thickness (μm)

Vehicle IMQ

PBS Monensin

e

Vehicle+PBS Vehicle+Monensin IMQ+PBS IMQ+Monensin

IL1f9 IL17c Ccl5 S100a8

Relative expression unit (IL1f9/Gapdh)_Δ Relative expression unit (IL17c/Gapdh) Relative expression unit (Ccl5/Gapdh) Relative expression unit (S100a8/Gapdh)

Supplementary Figure 5. Intraperitoneal injection of monensin ameliorates IMQ-induced psoriasis-like skin inflammation in mice. **a.** Macroscopic evaluation of vehicle- or IMQ-treated mice, with or without monensin injection, from day 1 to day 4. **b.** Mouse weight and skin scores represent skin thickness, erythema and scaling evaluation on vehicle or IMQ-treated mice with (n=8) or without monensin (n=7) injection. **c.** Toluidine blue staining and quantification of mouse skin with or without monensin treatment (n=7). **d.** H&E staining and quantification of epidermal thickness in vehicle- or IMQ-treated mouse skin (n=7). **e.** The expression of Il1f9, Il17c, Ccl5, and S100a8 was detected by qRT-PCR in vehicle- or IMQ-treated mice with (n=8) or without Monensin (n=7) injection. The data were analyzed by one-way ANOVA (**c-e**) and two-way ANOVA (**b**). Data are presented as mean \pm SD (**c-e**) or mean \pm SEM (**b**). Scale bar = 100 μ m. Source data are provided as a Source Data file.